Int. J. Electrochem. Sci., 14 **(2019)** 11663 – 11678, doi: 10.20964/2019.12.15

International Journal of
ELECTROCHEMICAL
SCIENCE
www.electrochemsci.org

Investigation of Mechanism of Tool Electrode Wear in Tube Electrode High-Speed Electrochemical Discharge Drilling

Yan Zhang[1,*], *Jian Tang*[1], *Yu Wang*[2], *Qin Ni*[1] *and Lei Ji*[1]

[1] School of Mechanical and Power Engineering, Nanjing Tech University, Nanjing 211800, PR China
[2] AECC Sichuan Gas Turbine Research Establishment, Sichuan 610500, PR China
[*]E-mail: zhangyanzy@njtech.edu.cn

Received: 3 July 2019 / *Accepted:* 2 September 2019 / *Published:* 29 October 2019

In tube electrode high-speed electrochemical discharge drilling (TSECDD), owing to electrical discharge erosion, tool electrode wear cannot be avoided and seriously affects the machining accuracy and efficiency of micro holes. To solve this problem, in this study, the mechanism of the tool electrode wear in TSECDD is investigated from three aspects: electrochemical reaming, gas film and sputtering layer. Moreover, a series of studies is conducted to identify the mechanism of the tool electrode wear in TSECDD. First, by comparing the tool electrode wear in electrical discharge machining (EDM) and TSECDD, it is found to be reduced by 14.75% when using TSECDD. By optimization experiments, it is then concluded that when the working fluid conductivity is 10 mS/cm, pulse width is 15 μs, pulse interval is 38 μs, and peak current is 8 A, the tool electrode wear is the least. Finally, the optimized parameters are used for hole machining, which proves that the improved tool electrode wear can effectively improve the machining performance of the hole.

Keywords: electrical discharge machining; electrochemical reaction; tool electrode wear; high-speed machining; micro holes

1. INTRODUCTION

Micro holes are widely used in aerospace manufacturing fields, and machining accuracy and surface quality can directly influence the performance and life of the components [1,2]. To machine a hole with a high machining speed, machining accuracy, and surface quality, tube electrode high-speed electrochemical discharge drilling (TSECDD) was proposed [3]. In this work, TSECDD and electrochemical machining are combined into one process. Owing to the effect of the electrical discharge erosion, tool electrode wear cannot be avoided in TSECDD. During electrical discharge machining (EDM), owing to the electrical discharge erosion, the tool electrode wear cannot be circumvented, and the machining accuracy of the workpiece is reduced [4]. Although TSECDD can realize efficient

machining of high-aspect-ratio features, the machining accuracy is considerably affected by the tool electrode wear, particularly during the electrical discharge erosion process. Therefore, to improve the surface quality and machining accuracy, it is important to study the wear mechanism of the tool electrode and reduce the tool electrode wear rate in TSECDD.

To analyse the mechanism of the tool electrode wear and reduce its influence on the machining performance, researchers have performed a tremendous amount of work. Mohri et al. [5] found that a precipitate on the surface of the tool electrode in EDM could effectively reduce its spark erosion. When the carbon content in the precipitate was high, the tool electrode wear was less. Marafona et al. [6] reported that a black layer composed of a bi-dimensional laminate of carbon crystals with random phases was formed on the surface of a tool electrode, which could effectively reduce the tool electrode wear. Bissacco et al. [7] proposed a method that could realize real-time online compensation by calculating the tool electrode wear and variation in the machining depth after the discharge in micro EDM. Lee et al. [8] conducted some research studies on electrode wear estimation and proposed a model in EDM drilling to estimate the tool electrode wear. Finally, the model could be used to estimate the electrode wear ratio within a 3% error margin. Maradia et al. [9] proposed that the thermal shielding due to low thermal conductivity of a diamond-like amorphous carbon and increased resistance to the abrasion owing to the high hardness of this layer resulted in a less electrode wear in meso–micro-EDM. Abou Ziki et al. [10] proposed a simplified lumped thermal model predicting tool expansion and its dynamics. Knowledge of the change in the tool length with time was helpful in improving the machining accuracy of micro-hole machining using spark-assisted chemical engraving. Behroozfar et al. [11] studied the effects of tool electrode materials on the tool electrode wear during the electrochemical discharge machining; the results verified that when the applied voltage was 50V, the surface temperature of the tool electrode would be increased to 2800℃, which could soften the tool electrode material and cause plastic deformation and accelerate the tool electrode wear. Kumar S.S et al. [12] proposed that adding SiC powder of average particle size 37 μm in the dielectric medium could reduce the rate of the tool electrode wear and improve the surface finish. Kumar M et al. [13] investigated the electro-discharge machining performance of Ti–6Al–4V alloy and found that the tool electrode wear rate reduced and surface roughness increased when changing the peak discharge current and pulse-on duration. Han et al. [14] investigated a combined process of EDM ablation and electrochemical machining (ECM) in an aerosol dielectric. In this process, the relative tool electrode wear rate decreased by 53.3%.

Different from the above-mentioned research studies, herein, the process of TSECDD includes not only electrical discharge erosion process, but also electrochemical dissolution process. Due to electrochemical reaction, the enlarged lateral gap is helpful to avoid the tool electrode wear generated by electrical discharge erosion. And the mechanism of tool electrode wear is also influenced by the gas film generated by electrochemical reaction. In addition, in the low-conductivity salt solution, a protective layer formed by sputtering is enhanced to compensate the tool electrode wear and improve the machining accuracy. In this study, first, the mechanism of the tool electrode wear in TSECDD was examined. Second, charge-coupled device (CCD) online observation and energy spectrum analysis were performed to confirm that a low-conductivity salt solution could reduce the wear of the tool electrode. Third, the optimal parameter combination was obtained by exploring the influence of the working fluid

conductivity, pulse width, pulse interval, and peak current on the tool electrode wear of TSECDD. The optimized parameters could further reduce the influences of the tool electrode wear on the machining performances.

2. EXPERIMENT METHODS

2.1 Mechanism of tool electrode wear in high-speed electrochemical discharge machining

In a high-speed electrochemical discharge machining process, the mechanism of the electrode wear can be analysed from three aspects: electrochemical reaming, gas film and sputtering layer. The mechanism of the tool electrode wear in high-speed electrochemcial discharge machining is shown in Fig. 1.

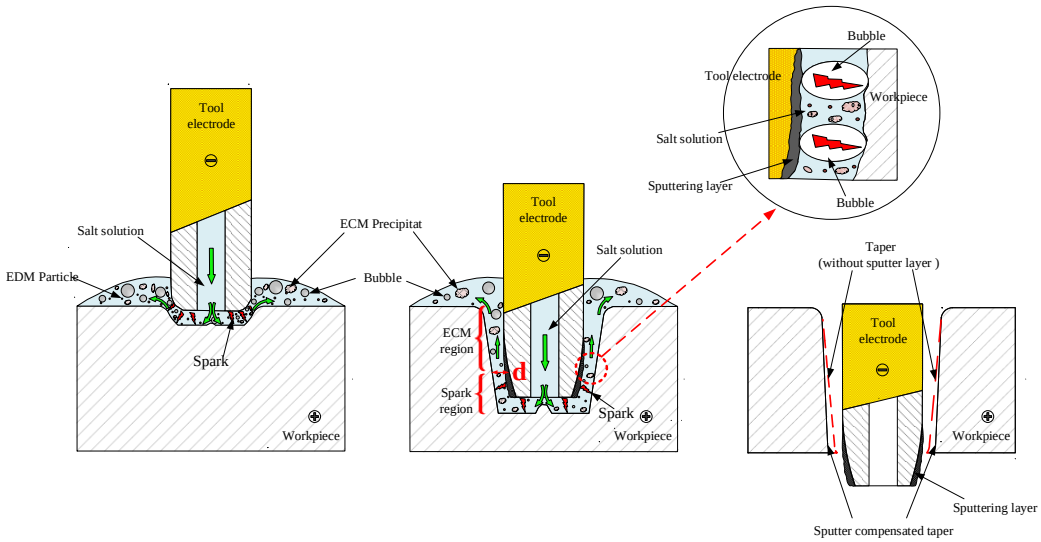

Figure 1. Mechanism of the tool electrode wear in high-speed electrochemical discharge machining.

2.1.1 Effect of electrochemical reaming

In the TSECDD process, the low-conductivity salt solution is used as the working fluid, electrical discharge erosion and electrochemical dissolution is simultaneously occurred in the lateral machining gap. Due to the electrochemical dissolution, with the drilling depth increasing, the lateral machining gap is gradually enlarged, and rapidly exceeds the critical distance of spark, especially for the region near the entrance. Thus, the electrical discharge machining stop in the lateral gap, which can avoid the erosion of the tool electrode material by electric sparking and reducing the tool electrode wear.

2.1.2 Effect of gas film on tool electrode wear

In a high-speed electrochemcial discharge machining process, sodium nitrate ($NaNO_3$) is used as the working fluid, and the electrochemical reaction equations are as follows:

At the anode:

The metal material can be dissolved as

$$Ni \rightarrow Ni^{2+} + 2e^{-}$$

Subsequently, the metal ions combine with the hydroxyl ions to precipitate as iron hydroxide,

$$Ni^{2+} + 2OH^{-} \rightarrow Ni(OH)_2 \downarrow$$

Hydroxyl ions evolve oxygen at the anode as

$$4OH^{-} \rightarrow O_2 \uparrow + 2H_2O + 4e^{-}$$

At the cathode:

The reaction is likely to be the generation of hydrogen gas and hydroxyl ions.

$$2H_2O + 2e^{-} \rightarrow 2OH^{-} + H_2 \uparrow$$

Therefore, in a hybrid process, numerous bubbles, such as of H_2 and O_2, can be generated by the electrochemical reaction. On the one hand, due to the large number of bubbles in the electrode gap, a gas film can be formed surrounding the end of the tool electrode, and the initial point and formation process of discharge channel are completed in the gas medium. The formation of discharge channel in TSECDD is similar to the breakdown of gas medium. Hence, compared with EDM in deionized water, the formation of discharge channel of TSECDD in the low-conductivity salt solution is easier and critical discharge gap is larger. Therefore, the electrode wear rate can be decreased. On the other hand, with the increase of the bubbles produced, the removal of the debris in the machining gap is accelerated and machining stability is improved, whereby the electrode wear from arc and the secondary discharge can be avoided and the electrode wear can also be reduced.

2.1.3 Effect of sputtering layer on tool electrode wear

Different from the EDM process with kerosene, in the process of high-speed electrochemcial discharge machining with sodium nitrate ($NaNO_3$), the high conductivity of the working fluid will increase the energy released by a single spark. This will cause a strong sputtering, and consequently, the molten debris is re-solidified and forms a covering layer on the surface of the tool electrode. Owing to the sputtering layer, the tool electrode wear can be effectively compensated.

2.2 Experimental equipment and procedure

2.2.1 Experimental equipment and materials

To further verify the mechanism of the tool electrode wear by experiments, an experimental system, as shown in Fig. 2, is designed; it includes a self-design fixture, power supply system, CCD observation cell, and voltage and current detecting system. The forming process of the bubbles and gas film in the machining gap is recorded by the CCD online observation system. Simultaneously, an oscilloscope is used to record the voltage and current signals throughout the process. By using this system, the whole machining process is analysed by observing the machining phenomenon and detecting the voltage and current waveforms.

The tool electrode used in the experiment is a brass tube electrode with an outer diameter of 0.5 mm and inner diameter of 0.2 mm. A nickel-based superalloy is used as the workpiece material with a thickness of 2 mm; it is commonly used to manufacture turbine blades and guide vanes owing to its excellent mechanical properties. The workpiece composition is listed in Table 1.

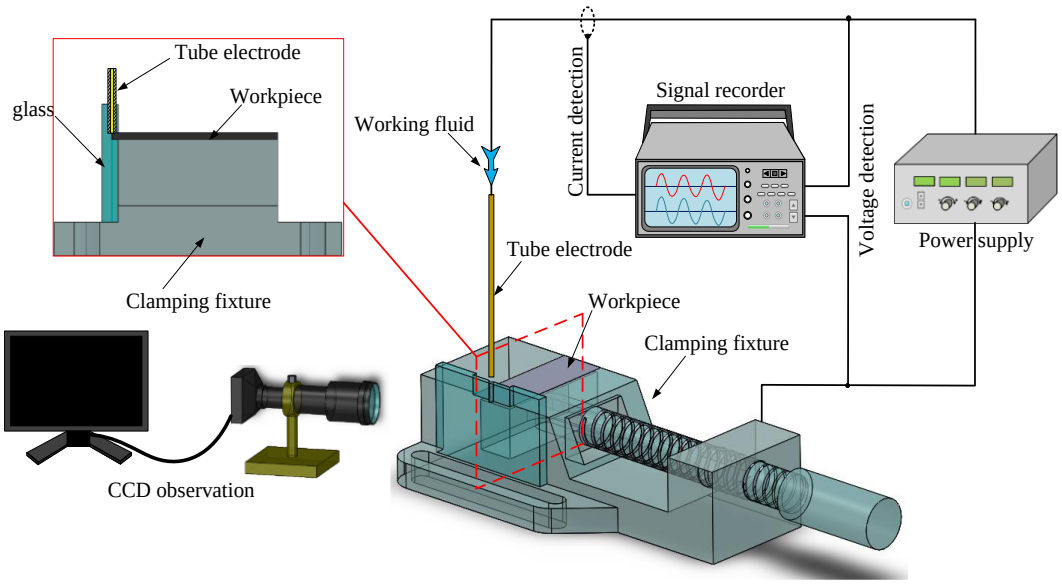

Figure 2. Schematic of the experimental system in high-speed electrochemical discharge machining.

Table 1. Elemental composition of the nickel-based superalloy

Element	Cr	Co	Mo	W	Re	Hf	Ta	Al	C	Si	Ni
Content	3.8～4.8	8.5～9.5	1.5～2.5	7.0～9.0	1.6～2.4	0.05～0.15	6.0～8.5	5.2～8.5	0.001～0.04	≤0.2	Bal.

2.2.2 Machining procedures and conditions

First, to confirm the mechanism of the tube electrode wear, comparison experiments are conducted between TSECDD and EDM. In this experiment, deionized water is used as the working fluid in the EDM process, whereas 3 mS/cm $NaNO_3$ solution is used as that in the TSECDD process. According to the previous studies reported by Zhang et al. [2], the other fixed parameters are listed in Table 2. Following the experiment, the morphology and composition of the end of the tube electrodes are compared and analysed. Second, for the TSECDD, the machining parameters, including the working fluid conductivity, pulse width, pulse interval, and peak current, are optimized. By the optimal experiments, the electrode wear is decreased, and the machining performance is enhanced. The machining parameters used in the optimal experiment are listed in Table 3. Finally, the optimized parameters are compared with the parameters without optimization. By comparing the relative electrode

wear rate (REWR), material removal rate (MRR), and taper of holes, it is confirmed that the optimized TSECDD can achieve reduced tool electrode wear and improve the machining performance of the hole machining.

Table 2. Parameter values used in the comparison experiments between TSECDD and EDM

	EDM	TSECDD
Working fluid	Deionized water	3 mS/cm $NaNO_3$ solution
Flushing pressure	4 MPa	4 MPa
Pulse width	12 μs	12 μs
Pulse interval	36 μs	36 μs
Peak current	12 A	12 A

Table 3. Machining parameters used in the optimal experiments

Experimental factor	Level					Other fixed parameters
Pulse width (μs)	3	6	9	12	15	Pulse interval: 38 μs Peak current: 8 A Working fluid conductivity: 10mS/cm $NaNO_3$
Pulse interval (μs)	6	14	22	30	38	Pulse width: 15 μs Peak current: 8 A Working fluid conductivity: 10 mS/cm $NaNO_3$
Peak current (A)	8	16	24	32	40	Pulse width: 15 μs Pulse interval: 38 μs Working fluid conductivity: 10mS/cm $NaNO_3$
Working fluid conductivity (mS/cm)	2	4	6	8	10	Pulse width: 15 μs Pulse interval: 38 μs Peak current: 8 A

2.2.3 Measurements and data acquisition

The inlet and outlet of the holes and end morphology of the tube electrode are observed via metallographic microscopy and scanning electron microscopy (SEM). The elemental composition of the tool electrode surface is detected by energy-dispersive X-ray spectroscopy. The effect of the tool electrode wear during TSECDD is evaluated based on the REWR and MRR in the length direction. The REWR is calculated by the following equation:

$$REWR = \frac{V_{electrode}}{V_{workpiece}} * 100\% \quad \text{..... (1)}$$

where Velectrode is the volume of the tool electrode wear and Vworkpiece is the volume of the hole machined by TSECDD.

Moreover, the MRR is given by the following equation:

$$MRR = \frac{L}{t} \quad \text{..... (2)}$$

where L is the machining depth and t is the drilling time. The MRR can be used to reflect the machining speed.

3. RESULTS AND DISCUSSION

3.1 Analysis of mechanism of tool electrode wear in TSECDD

The mechanism of the tool electrode wear is confirmed by comparative experiments between TSECDD and EDM. Moreover, the reasons of the tool electrode wear in TSECDD are elucidated from electrochemical reaming, the bubble film formation and the content of sputtering layer on the surface of the tool electrodes.

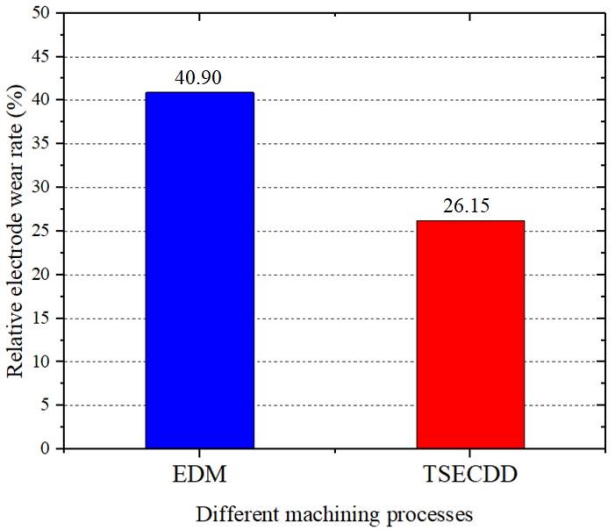

Figure 3. Comparison of the relative electrode wear rates of TSECDD and EDM.

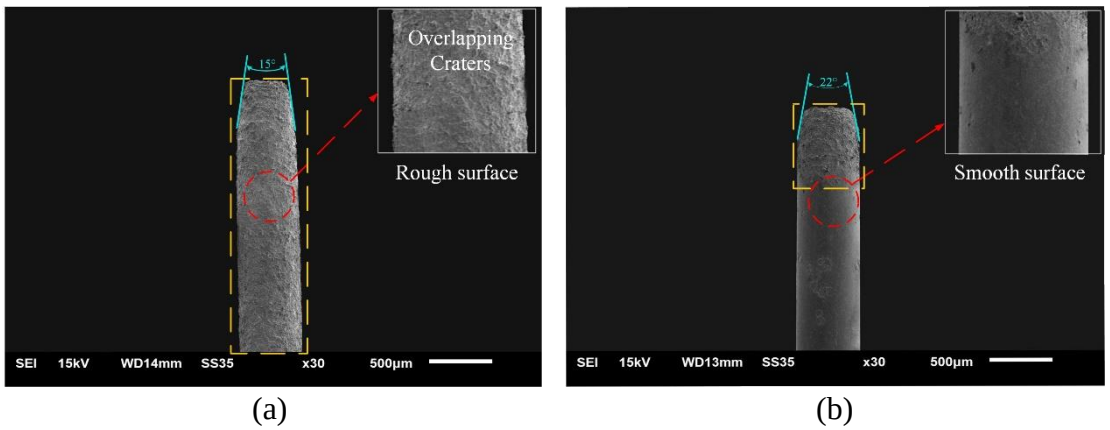

(a) (b)

Figure 4. Comparison of the tool electrode wear in different machining processes: (a) EDM was performed with deionized water, pulse width of 12 mS/s, pulse interval of 36 mS/s and peak current of 12 A. (b) TSECDD was performed with working fluid conductivity of 4 mS/cm, pulse width of 12 mS/s, pulse interval of 36 mS/s and peak current of 12 A.

Figure 3 shows the comparison of the REWRs of TSECDD and EDM. In the EDM process, the REWR is 40.90%, which is similar with the result of micro-EDM using copper electrode material, reported by Uhlmann [15].

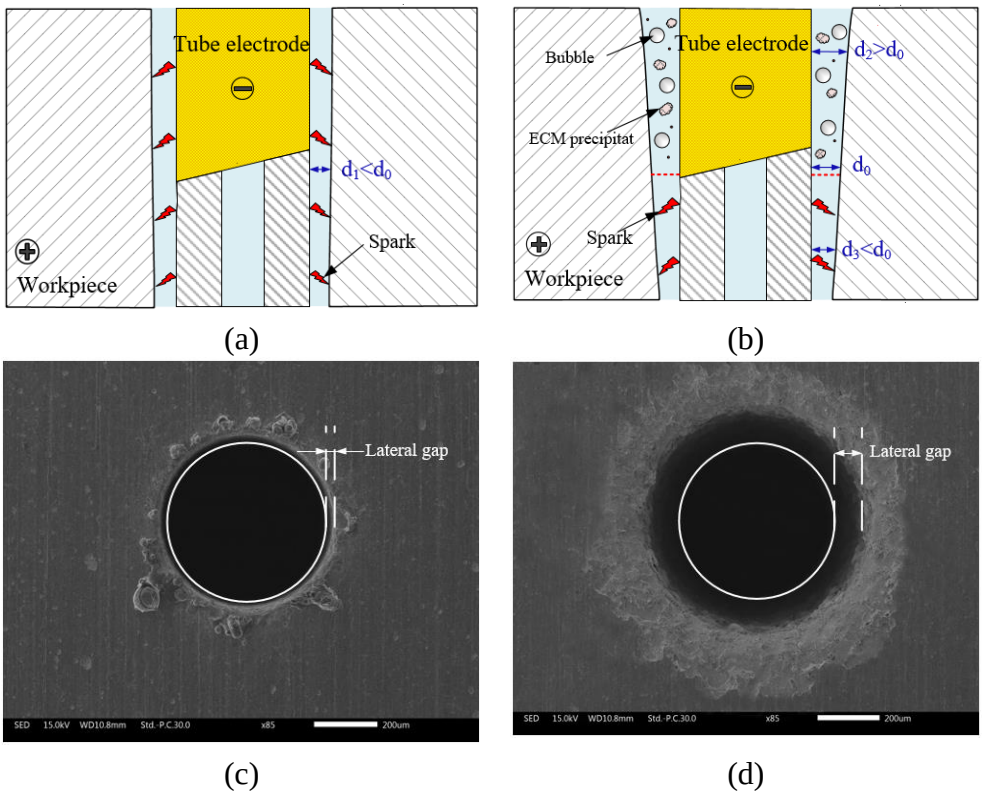

Figure 5. Comparison of lateral gap obtained in different machining processes: (a) The schematic diagram of lateral gap obtained in EDM. (b) The schematic diagram of lateral gap obtained in TSECDD. (c) Scanning electron micrograph of lateral gap of hole inlet in EDM was performed with deionized water, pulse width of 12 mS/s, pulse interval of 36 mS/s and peak current of 12 A. (d) Scanning electron micrograph of lateral gap of hole inlet in TSECDD was performed with working fluid conductivity of 4 mS/cm, pulse width of 12 mS/s, pulse interval of 36 mS/s and peak current of 12 A.

Whereas the tool electrode wear in SEDCM is lower than that in EDM, because the working fluid is made up with deionized water and triethanolamine in SEDCM, reported by Yin [16]. However, in the TSECDD process using low-conductivity salt solution, the REWR is reduced to 26.15%; therefore, the REWR of TSECDD is significantly lower than that of EDM. The tool electrode wear after EDM and TSECDD are shown in Fig. 4. In EDM, there are numerous electrical erosion craters on the entire surface of the tool electrode generated by high-temperature melting and a taper angle ($\theta = 15°$) at the end of the tool electrode, as shown in Fig. 4(a). When using TSECDD, as shown in Fig. 4(b), the area of the overlapping craters is significantly reduced on the surface of the tool electrode, and most of the surface of the tube electrode is relatively smooth. In addition, the taper angle generated by the tool electrode wear is increased to 22°. In TSECDD, the electrode wear occurs at the end of the electrode, and the REWR is evidently lower than that in EDM. Therefore, compared with pure EDM, the tool electrode

wear is significantly reduced in TSECDD, which is attributed to the electrochemical reaction. The distinct reasons can be explained from three aspects: electrochemical reaming, gas film and sputtering layer.

Figure 5 shows the comparison of lateral gap obtained in different machining processes. It can be seen that the lateral machining gap of the micro hole obtained in TSECDD is larger than that in EDM. This is because when the low-conductivity salt solution is used as the working fluid, the discharging and electrochemical dissolution are occurring simultaneously [17]. Due to the enlarging of lateral gap caused by electrochemical reaming, electrical discharge reaction gradually decreases in the lateral gap. It can be concluded that the electrochemical process in TSECDD makes much larger machining gap than that of EDM, which can avoid the erosion of the tool electrode material by the discharge and reducing the tool electrode wear.

Formation of a gas film in the EDM and TSECDD processes is observed, and the results are shown in Fig. 6. Based on Fig. 6(a), in the EDM process, where deionized water is used as the working fluid, bubbles are generated sporadically, and they adhere to the surface of the tool electrode irregularly. However, in the TSECDD process using $NaNO_3$ as the working fluid, numerous bubbles are generated on the tool electrode surface from the electrolyte, merge together, and evolve into a stable gas film, as shown in Fig. 6(b). When the $NaNO_3$ solution is used in TSECDD, an electrochemical reaction occurs and leads to the generation of numerous bubbles and formation of a gas film. Therefore, during the entire TSECDD process, the surface of the end of tool electrode is typically covered with a layer of bubbles, which makes it easy to form the discharge channel at a large distance. The stable discharge process can be effectively maintained by the stability of the gas film structure [18], thus in the large distance, the discharge energy concentrated on the surface of tool electrode is weakened and the tool electrode wear is greatly reduced. In addition, the stable gas film surrounding the end of the tool electrode accelerates the removal of the debris in the machining gap and reduces the abnormal discharge and secondary discharge; thus, the tool electrode wear can be reduced. Therefore, the electrode wear rate can be effectively decreased in TSECDD.

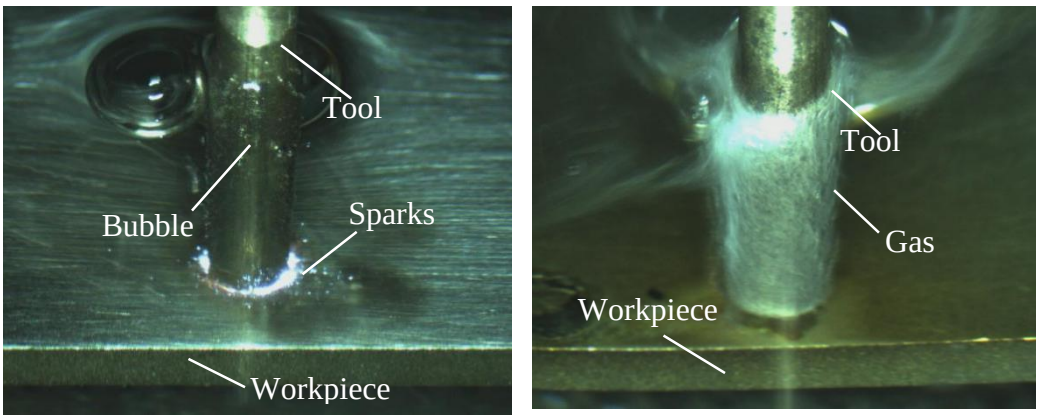

(a) (b)

Figure 6. Gas film formed in different processes: (a) EDM was performed with deionized water, pulse width of 12 mS/s, pulse interval of 36 mS/s and peak current of 12 A. (b) TSECDD was performed with working fluid conductivity of 4 mS/cm, pulse width of 12 mS/s, pulse interval of 36 mS/s and peak current of 12 A.

Figure 7 shows that, whether in EDM or TSECDD, part elements of the workpiece appear on the surface of the tool electrode. The results of the analysis of the elemental energy spectrum of the sputtering layer show that in EDM, the content of the workpiece elements in the sputtering layer is 47.71%, whereas in TSECDD, it is 70.19%. This is mainly because a sputtering phenomenon occurs in the electrical discharge erosion process. Different from the use of deionized water used in EDM, a low-conductivity salt solution is used as the working fluid in TSECDD. Thus, a single spark has a high energy, which can increase the probability of the sputtering of the workpiece materials in TSECDD. Therefore, the element content from the workpiece in the sputtering layer in TSECDD is higher than that in EDM. Concurrently, in the TSECDD process, the wear of the tool electrode can be effectively compensated by the sputtering layer, whereby the contour accuracy of the tool electrode can be improved.

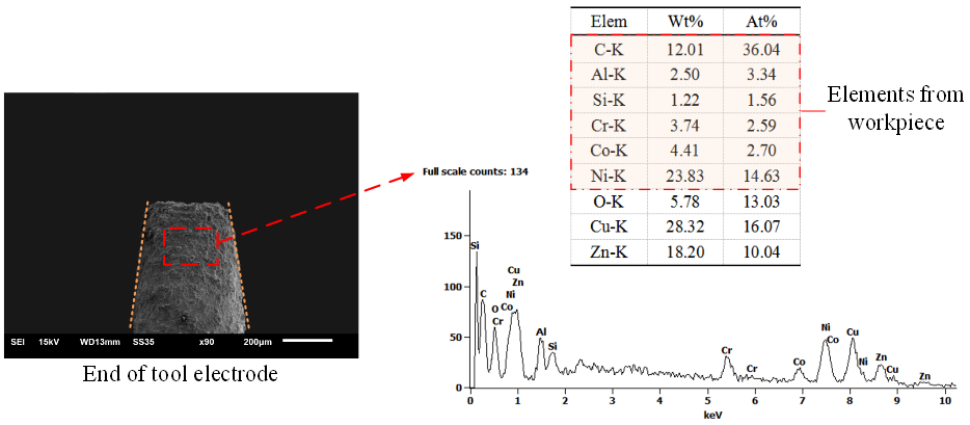

(**a**)

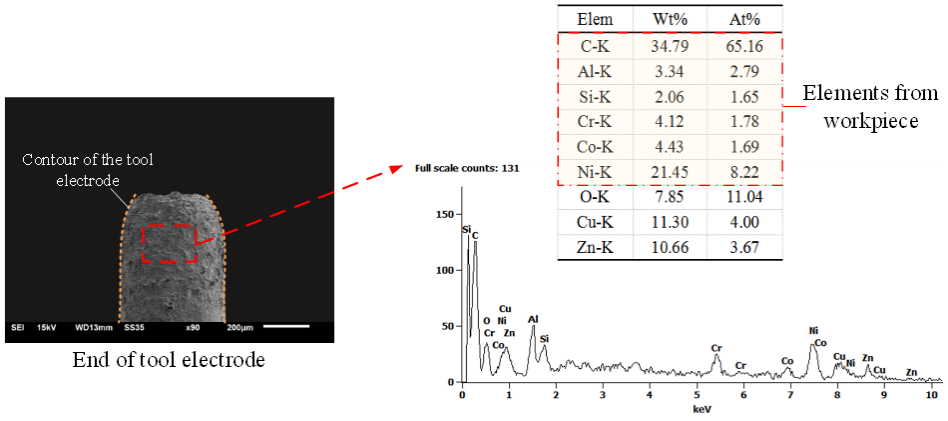

(b)

Figure 7. Elemental energy spectrum of the sputtering layer on the electrode surface generated by different processes: (a) EDM was performed with deionized water, pulse width of 12 mS/s, pulse interval of 36 mS/s and peak current of 12 A. (b) TSECDD was performed with working fluid conductivity of 4 mS/cm, pulse width of 12 mS/s, pulse interval of 36 mS/s and peak current of 12 A.

3.2 Effect of machining parameters on tool electrode wear

To improve the machining performance of the hole, the relationships between the machining parameters and tool electrode wear are studied.

3.2.1 Effect of working fluid conductivity on tool electrode wear

The variations in the REWR and processing time with the working fluid conductivity are shown in Fig. 8. As can be seen, with the increase in the working fluid conductivity, the REWR gradually reduces. Specifically, as the working fluid conductivity increases from 2 mS/cm to 10 mS/cm, the REWR reduces by 12.19%. This is because when the working fluid conductivity increases from 2 mS/cm to 10 mS/cm, the increase in the conductivity of the ions in the working fluid transforms the material removal mechanism from one mainly depending on the electrical discharge erosion to one mainly depending on the electrochemical dissolution in TSECDD. The above can also be illustrated by the variation in the processing time. Therefore, with the conductivity increasing, the electrical discharge erosion gradually weakens in this hybrid process, whereas the electrochemical reaction is gradually enhanced [19]. Thus, the enhanced electrochemical dissolution can increase the number of bubbles, accelerate the removal of the electrolysis product, and enhance the compensation of the sputtering layer, which can effectively reduce the wear of the tool electrode. In brief, the increase in the working fluid conductivity can effectively reduce the relative wear of the tool electrode. When the working fluid conductivity is 10 mS/cm, the wear of the tool electrode has little effect on the hole machining.

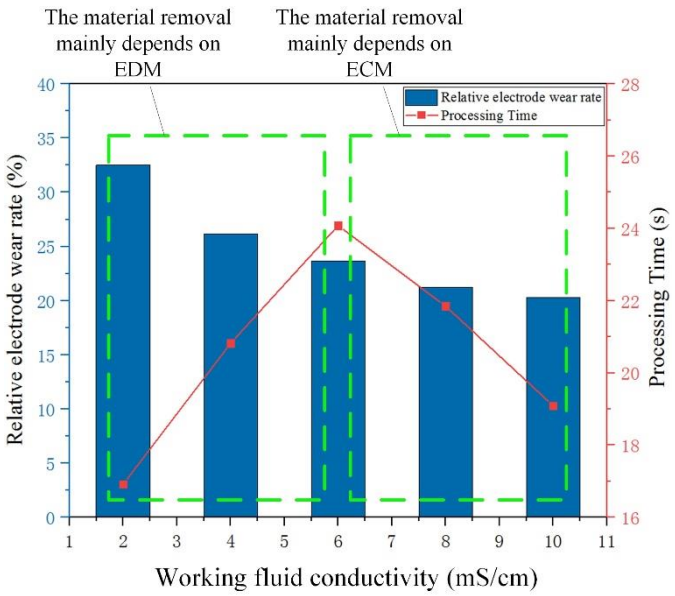

Figure 8. The bar chart of relative electrode wear rate and processing time line chart with working fluid conductivity of 2 mS/cm, 4 mS/cm, 6 mS/cm, 8 mS/cm, 10 mS/cm.

3.2.2 Effect of pulse width on tool electrode wear

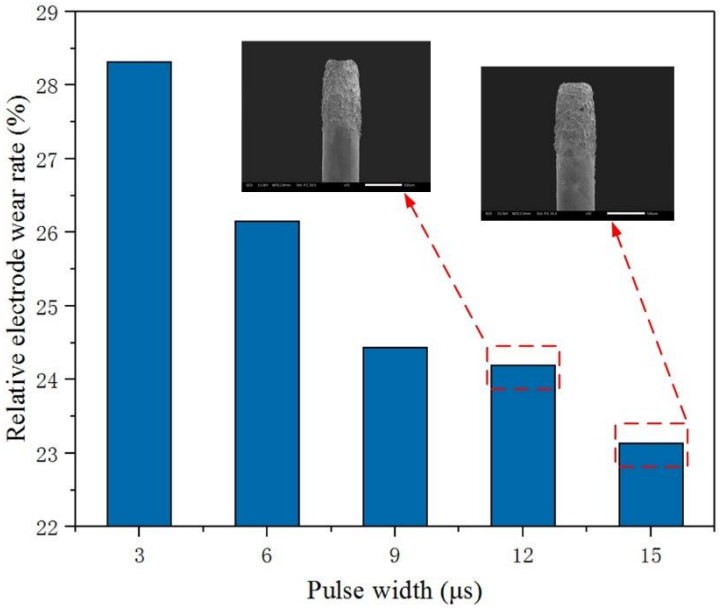

Figure 9. The bar chart of relative electrode wear rate with pulse width of 3 μs, 6 μs, 9 μs, 12 μs, 15 μs.

Figure 9 shows the effect of the pulse width on the REWR. With the increase in the pulse width, the relative electrode wear rate is gradually decreased. As the pulse width increases from 3 μs to 15 μs, the REWR of the tool electrode is reduced by 5.18%. This can be understood because with the pulse width increase, the electrochemical reaction is enhanced in TSECDD. Thus, the volume of the hole machined by TSECDD is more enlarged, and the REWR is reduced. Concurrently, an enhanced electrochemical reaction is more conducive to the formation of a stable gas film, which is helpful in protecting the tool electrode from wear. By contrast, with the increase of the pulse width, the discharge energy of a single pulse increases [20]. Thus, the materials of the workpiece and electroerosion product sputtering on the surface of the tool electrode increase, and the compensation effect of the covering layer on the tool electrode wear is gradually enhanced. According to the above analysis, with pulse width increase, the tool electrode wear is generally reduced in the TSECDD process. When the pulse width is 15 μs, minimum wear of the tool electrodes can be obtained in TSECDD.

3.2.3 Effect of pulse interval on tool electrode wear

Figure 10 shows the effect of the pulse interval on the REWR; with the increase in the pulse interval, the REWR generally decreases. When the pulse interval is large, the REWR is low. This can be understood because with the increase in the pulse interval, the number of pulse discharges per unit time decreases, so that the energy of the electrical spark decreases and electrode wear reduces. In addition, owing to the increase of the pulse interval, the ratio of the electrical discharge erosion in the hybrid machining is reduced [21], whereas the electrochemical dissolution becomes the main machining process in TSECDD. Hence, as the electrochemical dissolution enhances, the number of bubbles generated gradually increases, which accelerates the formation of a gas film and removal of the

machining products in the interelectrode, whereby reducing the wear of the tool electrode. Therefore, to obtain a low REWR, the pulse interval should be selected to have a value larger than 38 μs.

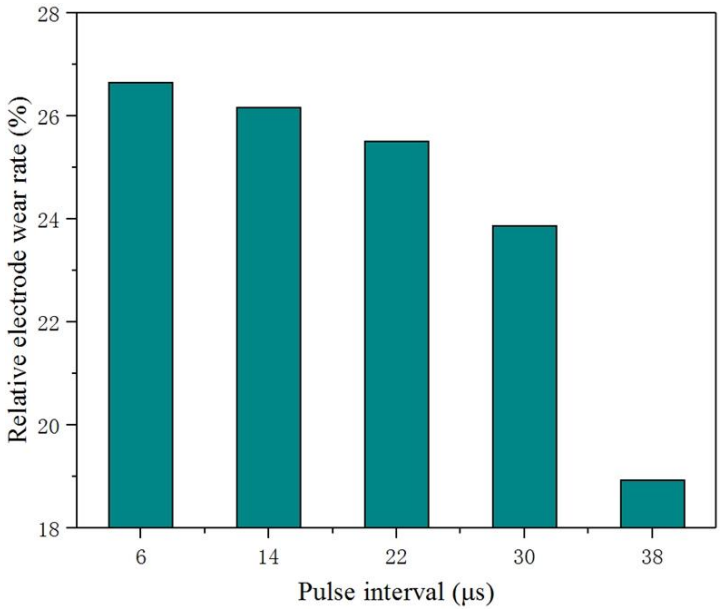

Figure 10. The bar chart of relative electrode wear rate with pulse interval of 6 μs, 14 μs, 22 μs, 30 μs, 39 μs.

3.2.4 Effect of peak current on tool electrode wear

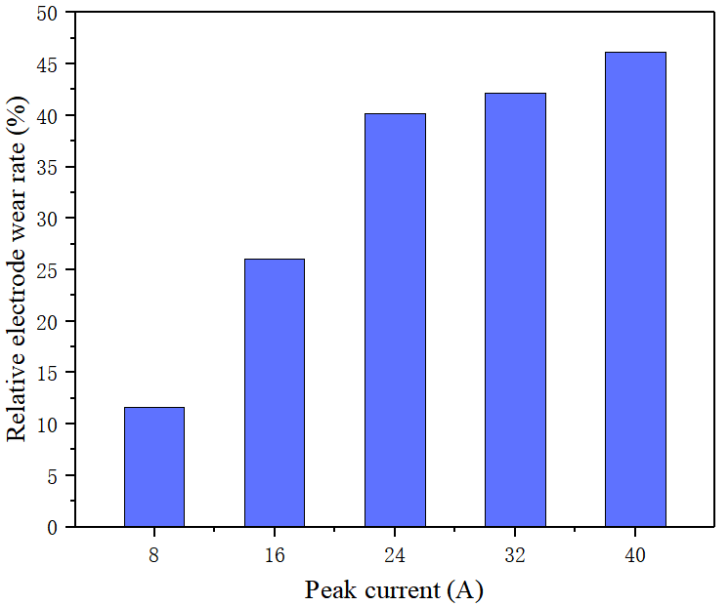

Figure 11. The bar chart of relative electrode wear rate with peak current of 8 A, 16 A, 24 A, 32 A, 40 A.

Figure 11 reveals the effect of the peak current on REWR and processing time. With increasing peak current (7–24 A), the REWR increases linearly. This can be explained in that with the increase in the peak current, the discharge energy of a single pulse increases, resulting in a simultaneous increase in the material wear of the tool electrode when the spark breaks through the machining gap. As the peak current continues to increase (24–40 A), the rate of increase in the relative electrode wear rate begins to decrease. By observing the morphology of the end of the tool electrode, with further increase in the peak current (24–40 A), the sputtered material on the surface of the tool electrode is increased, which leads to increased compensation of the tool electrode wear. Concurrently, because the electrochemical dissolution is gradually enhanced, the amount of bubble is increased, which further accelerates the removal of the electrochemical products in the narrow gap and improves the stability of the discharge [22]. Consequently, the rate of increase in the relative wear of the tool electrode begins to decrease. In summary, combining the experimental results of the tool electrode wear, the optimal peak current should be 8 A.

Based on the results presented in Figs. 8-11, when the working fluid conductivity is 10 mS/cm, pulse width is 15 μs, pulse interval is 38 μs, and peak current is 8 A, the machining process is associated with a less tool electrode wear but with a high machining efficiency.

3.3 Improvement in machining performance by using optimized parameters

Figure 12 presents a comparison of the REWR and MRR during the hole machining of a cobalt-based superalloy by TSECDD with and without the optimization parameters.

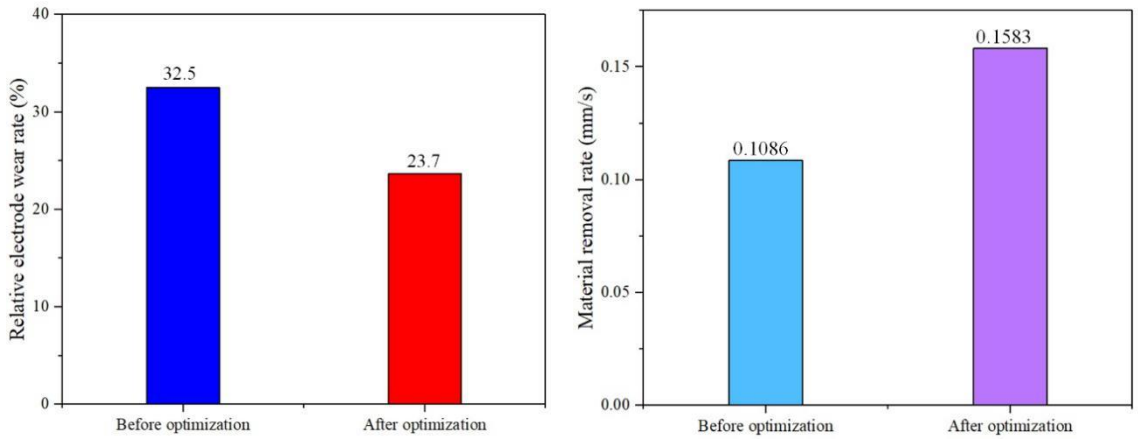

(a) (b)

Figure 12. Comparison of the REWR and MRR using TSECDD obtained both with the optimized parameters: working fluid conductivity is 10 mS/cm, pulse width is 15 μs, pulse interval is 38 μs, peak current is 8 A. and the parameters before optimization: the working fluid conductivity is 4 mS/cm, pulse width is 12 μs, pulse interval is 36 μs, peak current is 12 A. (a) Relative electrode wear rate. (b) Material removal rate.

Figure 12(a) shows that the REWR after optimization is 23.7%, lower than 32.5% that that when using common parameters without optimization. Further, Fig. 12(b) shows that the MRR after optimization is 0.1583 mm/s, higher than 0.1086 mm/s versus the MRR before optimization. By using the optimization parameters, the REWR can be effectively reduced, whereas the MRR can be improved. The low tool electrode wear and high sputtering layer compensation can further improve the MRR.

Figure 13 displays a comparison of the geometric morphology of the hole machined by TSECDD with and without the optimization parameters. Figures 13 (a) and (b) show that the taper angle is reduced from 9° to 6° by the electrode wear optimization, which can prove that owing to the optimization of the machining parameters, the electrode wear can be decreased. Thus, high-efficiency sputter layer compensation can effectively reduce the taper angle of the holes, and thereby further improve the machining precision of the holes.

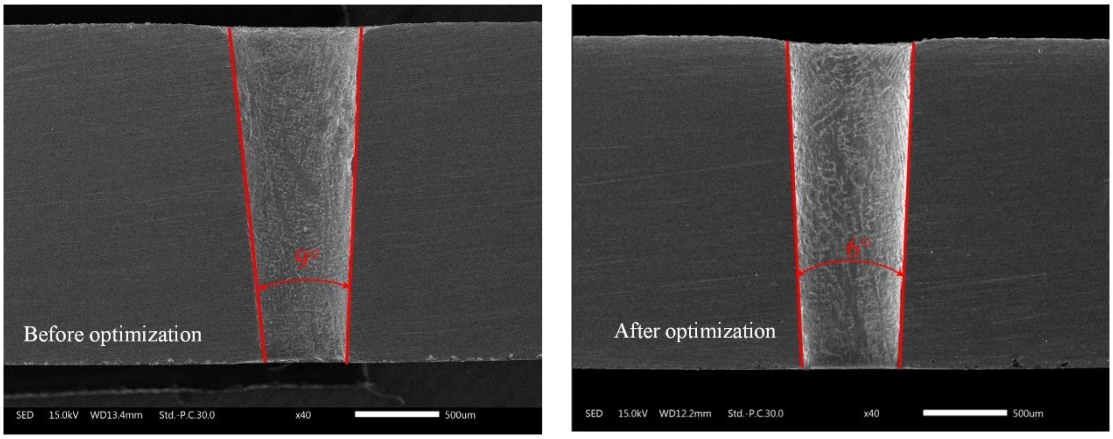

(**a**) (**b**)

Figure 13. Comparison of the geometric morphology after TSECDD: (a) Scanning electron micrograph of the geometric morphology with the parameter before optimization：the working fluid conductivity is 4 mS/cm, pulse width is 12 μs, pulse interval is 36 μs, peak current is 12 A. (b) Scanning electron micrograph of the geometric morphology with the optimized parameter： working fluid conductivity is 10 mS/cm, pulse width is 15 μs, pulse interval is 38 μs, and peak current is 8 A.

4. CONCLUSIONS

In this study, the mechanism of tool electrode wear is analysed and machining parameters are optimized and used to improve the machining accuracy and machining efficiency of micro holes. The main findings of the study can be summarized as follows:

(1) The mechanism of the tool electrode wear in TSECDD is investigated from three aspects: electrochemical reaming, gas film and sputtering layer. It is found that electrochemical reaming, a stable gas film and sputtering layer can be used to protect the tool electrode from the electrical discharge erosion.

(2) By the optimization experiment of TSECDD, it is concluded that when the working fluid conductivity is 10 mS/cm, pulse width is 15 μs, pulse interval is 38 μs, and peak current is 8 A, the tool electrode wear can realize the optimal value.

(3) The relative electrode wear rate is reduced to 23.7% by the optimization of the parameters. The material removal rate after optimization is increased to 0.1583 mm/s, and the taper angle of the hole is reduced from 9° to 6° by the electrode wear optimization.

ACKNOWLEDGEMENTS
This project is supported by the National Natural Science Foundation of China (Grant No. 51705239).

References

1. S.Z. Chavoshi and X. Luo, *Precis. Eng.*, 41 (2015) 1.
2. M. Goiogana and A. Elkaseer, *Materials*, 12 (2019) 989.
3. Y. Zhang, Z.Y. Xu, D. Zhu and J. Xing, *Int. J. Mach Tools Manuf.*, 92 (2015) 10.
4. J. Murray, D. Zdebski and A.T. Clare, *J. Mater. Process. Technol.*, 212 (2012) 1537.
5. N. Mohri, M. Suzuki, M. Furuya, N. Saito and A. Kobayashi, *CIRP An. Manuf. Technol.*, 44 (1995) 165.
6. J. Marafona, *J. Mater. Process. Technol.*, 184 (2007) 27.
7. G. Bissacco, G. Tristo, H.N. Hansen and J. Valentincic, *CIRP An. Manuf. Technol.*, 62 (2013) 179.
8. C.S. Lee, E.Y. Heo, J.M. Kim, I.H. Choi and D.W. Kim, *Robot. Comput.-Integr. Manuf.*, 36 (2015) 70.
9. U. Maradia, M. Boccadoro, J. Stirnimannc, F. Kuster and K. Wegener, *J. Mater. Process. Technol.*, 223 (2015) 22.
10. J.D. Abou Ziki and R. Wuethrich, *Int. J. Adv. Manuf. Technol.*, 61 (2012) 481.
11. A. Behroozfar and M.R. Razfar, *Mater. Manuf. Processes*, 31 (2016), 574.
12. S.S. Kumar, J. Thrinadh, D. Saurav and N. Goutam, *J. Braz. Soc. Mech. Sci. Eng.*, 40 (2018) 330.
13. M. Kumar, S. Datta and R. Kumar, *Arabian J. Sci. Eng.*, 44 (2019) 1553.
14. Y.X. Han, Z.D. Liu, Z.L. Cao, L.L. Kong and M.B. Qiu, *J. Mater. Process. Technol.*, 254 (2018) 221.
15. E. Uhlmann and M. Roehner, *CIRP J. Manuf. Sci. Technol.*, 1 (2008) 92.
16. Q.F. Yin, B.R. Wang, Y.B. Zhang, J. Fang and G.M. Liu, *J. Mater. Process. Technol.*, 214 (2014) 1759.
17. M. Goud, A.K. Sharma and C. Jawalkar, *Precis. Eng.*, 45 (2016) 1.
18. C.P. Cheng, K.L. Wu, C.C. Mai, C.K. Yang, Y.S. Hsu and B.H. Yan, *Int. J. Mach Tools Manuf.*, 50 (2010) 689.
19. V.G. Ladeesh and R. Manu, *J. Braz. Soc. Mech. Sci. Eng.*, 40 (2018) 19.
20. B. Hardik and P.M. Pandey, *J. Manuf. Process.*, 34 (2018) 356.
21. X.J. Tian, Y.H. Liu, B.P. Cai, R.J. Lin, Z.K. Liu and R. Zhang, *Int. J. Adv. Manuf. Technol.*, 66 (2013) 1673.
22. S. Kumar, A. Batish, R. Singh and A. Bhattacharya, *Wear*, 386-387 (2017) 223.